DOI: http://dx.doi.org/10.12989/sem.2010.34.2.143

Stress concentrations around a circular hole in an infinite plate of arbitrary thickness

Longchao Dai† and Xinwei Wang

Institute of Structure and Strength, Nanjing University of Aeronautics and Astronautics, Nanjing 210016, P.R. China

Feng Liu

College of Aviation Engineering, Civil Aviation Flight University of China, Guanghan, 618307, P.R. China

(Received April 15, 2008, Accepted November 4, 2009)

Abstract. This paper presents theoretical solutions for the three-dimensional (3D) stress field in an infinite isotropic elastic plate containing a through-the-thickness circular hole subjected to far-field in-plane loads by using Kane and Mindlin's assumption. The dangerous position, where the premature fracture or failure of the plate will take place, the expressions of the tangential stress at the surface of the hole and the out-of-plane stress constraint factor are found in a concise, explicit form. Based on the present theoretical solutions, a comprehensive analysis is performed on the deviated degree of the in-plane stresses from the related plane stress solutions, stress concentration and out-of-plane constraint, and the emphasis has been placed on the effects of the plate thickness, Poisson's ratio and the far-field in-plane loads on the stress field. The analytical solution shows that the effects of the plate thickness and Poisson's ratio on the deviation of the 3D in-plane stress components is obvious and could not be ignored, although their effects on distributions of the in-plane stress components are slight, and that the effect of the far-field in-plane loads is just on the contrary of that of the above two. When only the shear stress is loaded at far field, the stress concentration factor reach its peak value about 8.9% higher than that of the plane stress solutions, and the out-of-plane stress constraint factor can reach 1 at the surface of the hole and is the biggest among all cases considered.

Keywords: three-dimensional stress field; through-the-thickness circular hole; thickness effect; stress concentration; out-of-plane constraint.

1. Introduction

It is well recognized that stress concentration, which has long been a concern, is a very important phenomenon to cause premature fracture or failure of materials and structures. Fortunately, it has been confirmed by several numerical computations that the corresponding plane solutions of the theory of elasticity provide a good approximation to the in-plane stress. For example, the plane

† Corresponding author, E-mail: dai_lc@163.com

stress assumptions, i.e., the out-of-plane stresses are negligible as compared to the in-plane ones, can be used to study deformations of thin plates under in-plane loads. Consequently, in many analyses on practical problems including plasticity problem (e.g., Dugdale model in fracture mechanics), the plane stress solution is still acceptable to study the stress field in a plate with thickness of at least an order of magnitude smaller than a characteristic in-plane dimension. However, strictly speaking, plane solutions of the theory of elasticity are only valid for plates with vanishing thickness or infinite thickness where the stress state can be classified as plane-stress or plane-strain, respectively. Furthermore, it is also recognized that these plane solutions are not applicable when assessing the out-of-plane stress and deformation (Sternberg and Sadowsky 1949, Young and Sternberg 1966, Folias and Wang 1990, Krishnaswamy *et al.* 1998, Li *et al.* 2000). For its importance, a lot of efforts have been paid to make clear of 3D stress field in a plate based on the theoretical and numerical studies, since the exact analysis is mathematically difficult to develop.

Recently, much attention has been paid to study on the two-dimensional and three-dimensional (3D) stress field in the vicinity of a circular hole/inclusion (Chaudhuri 2003a, b, Folias and Wang 1990, Krishnaswamy *et al.* 1998, Kotousov and Wang 2002b, Penado and Folias 1989, Yang *et al.* 2008), a crack (Folias 1975, Jin and Hwang 1989, Jin and Batra 1997, Kotousov 2007, Kotousov and Wang 2002c, Yang and Guo 2005, Yang and Freund 1985) and a notch (Filippi *et al.* 2002, Filippo *et al.* 2004, Kotousov and Wang 2002a, Lazzarin and Tovo 1996, Li and Guo 2001, Li *et al.* 2000). However, the effects of the plate thickness, Poisson's ratio and the loads on the stress field, the deviated degree of the in-plane stresses from the related plane stress solutions, the stress concentration and out-of-plane constraint have not been performed comprehensively for the case of a finite thickness plate.

Because of the difficulty in satisfying boundary conditions precisely, there are only a few analytical 3D solutions available in the literature for relatively simple configurations with favorable conditions of symmetry. About sixty years ago, by the use of series expansion and taking finite terms into account, an excellent approximate solution for 3D stress distributions in the neighborhood of a circular hole in an infinite plate of arbitrary thickness is obtained by Sternberg and Sadowsky (1949). Detailed analyses for the out-of-plane stress constraint were provided, but for stress concentrations only a brief discussion was given. By a similar method, the stress distribution near a general triaxial ellipsoidal cavity in an infinite elastic body subjected to a triaxial tension is obtained by Sadowsky and Sternberg (1949). Later, Kane and Mindlin (1956) provided a method to obtain 3D stress field, while still retaining the simplicity of a two-dimensional model. The method was employed by Yang and Freund (1985) and Jin and Hwang (1989) to study the effect of transverse shear on the stress field in an elastic plate containing a through-thickness crack. Recently, by using Kane and Mindlin's assumption, Jin and Batra (1997) analyzed the interface fracture of an elastic plate bonded to a rigid substrate and obtained the solutions of stresses and deformations for a semi-infinite plate perfectly bonded to a rigid substrate and subjected to uniform in-plane normal tractions at infinity. Using the same assumption, Krishnaswamy *et al.* (1998) investigated the stress concentration in elastic Cosserat plates with a circular hole undergoing extensional deformations. Unfortunately, some of the results are incorrect in their paper (Li *et al.* 2000 and Kotousov and Wang 2002a, b). More recently, Kotousov (2007), Kotousov and Wang (2002a, b, c, 2003) studied the 3D stress distribution around a notch, a circular hole or a crack in an isotropic elastic plate or a transversally isotropic elastic plate by using Kane and Mindlin's assumption. However, the explicit expressions for stress concentration and out-of-plane constraint factor in a plate with a circular hole have not been provided.

It is the purpose of this paper to present exact 3D solutions for the stress field in an infinite plate holding a through-the-thickness circular hole subjected to remote in-plane loads based on Kane and Mindlin's assumption. Explicit expressions for the tangential stress at the hole and the out-of-plane stress constraint factor are obtained in a concise, explicit form. Based on the present theoretical solutions, a comprehensive analysis is performed on the characters of 3D stress field, stress concentration and out-of-plane constraint, and the emphasis has been placed on the effects of the plate thickness, Poisson's ratio and the far-field in-plane loads on in-plane stress field, stress concentration and out-of-plane constraint.

2. Governing equations and the boundary conditions

Consider a homogeneous, isotropic, elastic, infinite plate bounded by planes $z = \pm h$ with a through-the-thickness circular hole in its center. The plate is subjected to in-plane loads, σ_x^∞, σ_y^∞ and τ_{xy}^∞, at infinite. Kane and Mindlin's kinematic assumption is adopted, namely, the displacement field in the plate has the following form

$$u_x = u(x,y)\,,\quad u_y = v(x,y)\,,\quad u_z = \frac{z}{h}w(x,y) \tag{1}$$

It is clear that Eq. (1) implies that lines normal to the mid-plane of the plate in the un-deformed state are still the normal in the deformed state and that these lines experience uniform extensional strain $w(x, y)/h$ along the z direction, where $w(x, y)$ is the out-of-plane displacement of the plate at $z = h$. With the displacement field given by Eq. (1), two out-of-plane shear stress components are linearly distributed in the thickness (z) direction.

Considering the following definitions

$$\begin{aligned}(\bar{\sigma}_{\alpha\beta}, \bar{\sigma}_{zz}, \bar{\kappa}_{z\beta}) &= \frac{1}{2h}\int_{-h}^{h}(\sigma_{\alpha\beta}, \sigma_{zz}, z\sigma_{z\beta})dz\\ (\bar{\varepsilon}_{\alpha\beta}, \bar{\varepsilon}_{zz}, \bar{\xi}_{z\beta}) &= \frac{1}{2h}\int_{-h}^{h}(\varepsilon_{\alpha\beta}, \varepsilon_{zz}, 2z\varepsilon_{z\beta})dz\end{aligned} \tag{2}$$

the constitutive relations and the equilibrium equations can be expressed as

$$(\bar{\varepsilon}_{\alpha\beta}, \bar{\varepsilon}_{zz}, \bar{\xi}_{z\beta}) = \frac{1+\nu}{E}(\bar{\sigma}_{\alpha\beta}, \bar{\sigma}_{zz}, 2\bar{\kappa}_{z\beta}) - \frac{\nu}{E}\bar{\sigma}_{kk}(\delta_{\alpha\beta}, 1, 0) \tag{3}$$

$$\bar{\sigma}_{\alpha\beta,\beta} = 0\,,\quad \bar{\kappa}_{z\beta,\beta} - \bar{\sigma}_{zz} = 0 \tag{4}$$

where E and ν are the Young's modulus and Poisson's ratio of an isotropic material. A comma stands for differentiation and repeated indices k implies summation. In Eqs. (2)-(4) and throughout the remains of the paper, Greek indices range 1 and 2. Introduce function ϕ, similar to the Airy stress-resultant function, and φ, and

$$\bar{\sigma}_{\alpha\beta} = \nabla^2\phi\delta_{\alpha\beta} - \phi_{,\alpha\beta},\quad \bar{\kappa}_{z\beta} = \varphi_{,\beta} \tag{5}$$

Thus, the first equation of Eq. (4) is automatically satisfied and the second equation of Eq. (4) can be simplified as

$$\bar{\sigma}_{zz} = \nabla^2\varphi \tag{6}$$

Inserting Eqs. (3), (5) and (6) into the deformed harmonious equations yields

$$\nabla^4\varphi = A\nabla^2\varphi, \quad \nu\nabla^2\phi = \nabla^2\varphi - A_2\varphi \tag{7}$$

where ∇^2 and ∇^4 are the two-dimensional Laplacian and biharmonic operators, respectively, and

$$A_2 = \frac{6(1+\nu)}{h^2}, \quad A = \frac{A_2}{1-\nu^2} \tag{8}$$

Introduce polar coordinates (r, θ). The formulae of stress components are

$$\bar{\sigma}_r = \frac{1}{r}\frac{\partial\phi}{\partial r} + \frac{1}{r^2}\frac{\partial^2\phi}{\partial\theta^2}, \quad \bar{\sigma}_\theta = \frac{\partial^2\phi}{\partial r^2}, \quad \bar{\sigma}_{r\theta} = -\frac{1}{r}\frac{\partial^2\phi}{\partial r\partial\theta} + \frac{1}{r^2}\frac{\partial\phi}{\partial\theta} \tag{9}$$

$$\bar{\sigma}_{zz} = \nabla^2\varphi, \quad \bar{\kappa}_{zr} = \frac{\partial\varphi}{\partial r}, \quad \bar{\kappa}_{z\theta} = \frac{1}{r}\frac{\partial\varphi}{\partial\theta}$$

In the polar coordinate systems, the boundary conditions can be expressed as follows

$$\begin{aligned}
\bar{\sigma}_r &= \frac{\sigma_x^\infty + \sigma_y^\infty}{2} + \frac{\sigma_x^\infty - \sigma_y^\infty}{2}\cos 2\theta + \tau_{xy}^\infty \sin 2\theta \\
\bar{\sigma}_\theta &= \frac{\sigma_x^\infty + \sigma_y^\infty}{2} - \frac{\sigma_x^\infty - \sigma_y^\infty}{2}\cos 2\theta - \tau_{xy}^\infty \sin 2\theta \\
\bar{\sigma}_{r\theta} &= -\frac{\sigma_x^\infty - \sigma_y^\infty}{2}\sin 2\theta + \tau_{xy}^\infty \cos 2\theta \quad (r \to \infty) \\
\bar{\sigma}_r &= 0, \quad \bar{\sigma}_{r\theta} = 0, \quad \bar{\kappa}_{zr} = 0 \qquad (r = R)
\end{aligned} \tag{10}$$

3. The stress solutions in a plate with a circular hole

Considering the boundary conditions (10), solutions to (7) can be found as

$$\begin{aligned}
\varphi(r,\theta) = &\left(c_{10} + c_{20}\ln r + c_{30}K_0(\sqrt{A}r)\right) + \left(c_{11}r^2 + c_{21}r^{-2} + c_{31}K_2(\sqrt{A}r)\right)\sin 2\theta \\
&+ \left(c_{12}r^2 + c_{22}r^{-2} + c_{32}K_2(\sqrt{A}r)\right)\cos 2\theta
\end{aligned} \tag{11}$$

$$\begin{aligned}
\phi(r,\theta) = &\left[d_{10} + d_{20}\ln r + \frac{A_2}{4\nu}c_{10}r^2 - \frac{A_2c_{20}}{4\nu}r^2(\ln r - 1) + \frac{A - A_2}{A\nu}c_{30}K_0(\sqrt{A}r)\right] \\
&+ \left[d_{11}r^2 + d_{21}r^{-2} - \frac{A_2c_{11}}{12\nu}r^4 + \frac{A_2}{4\nu}c_{21} + \frac{A - A_2}{A\nu}c_{31}K_2(\sqrt{A}r)\right]\sin 2\theta \\
&+ \left[d_{12}r^2 + d_{22}r^{-2} - \frac{A_2c_{12}}{12\nu}r^4 + \frac{A_2}{4\nu}c_{22} + \frac{A - A_2}{A\nu}c_{32}K_2(\sqrt{A}r)\right]\cos 2\theta
\end{aligned} \tag{12}$$

Inserting Eqs. (11) and (12) into Eq. (9), and considering the boundary conditions Eq. (10) and that all stress components must remain bounded at infinity, the solutions of all stress components are obtained, whose expressions are given in Appendix.

Then, the tangential stress at the surface of the hole can be expressed as follows

$$\bar{\sigma}_\theta\Big|_{r=R} = \sigma_x^\infty + \sigma_y^\infty + \frac{\left(\sigma_x^\infty - \sigma_y^\infty\right)\cos 2\theta + 2\tau_{xy}^\infty \sin 2\theta}{2} \cdot \left(-1 + \frac{c_{31}}{\tau_{xy}^\infty} \cdot \frac{A - A_2}{4\nu}\left(K_0 + 2K_2 + K_4\right) + \frac{d_{21}}{\tau_{xy}^\infty} \cdot \frac{6}{R^4}\right) \tag{13}$$

In Eq. (13) and throughout the remained paper, K_n denotes $K_n(\sqrt{A}R)$, the modified Bessel functions of order n, where n is an integer. Throughout the remains of the paper, the notation $\sigma_{\max}^\infty = \max(\sigma_x^\infty, \sigma_y^\infty, \tau_{xy}^\infty)$ is used. Consider the following definitions

the far-field in-plane loads ratio: $\sigma_x^\infty : \sigma_y^\infty : \tau_{xy}^\infty$

the tangential stress ratio: $K = \bar{\sigma}_\theta / \sigma_{\max}^\infty$

the stress concentration factor: $K_t = (\bar{\sigma}_\theta / \bar{\sigma}_0)\big|_{r = R,\, \theta = \theta_t}$

Where θ_t is at the location where $\bar{\sigma}_\theta\big|_{r=R}$ reaches its peak value and can be determined by Eq. (13), namely

$$\theta_t = \frac{1}{2}\arctan t + \frac{\pi}{2} \qquad (\theta_t \in [0, 2\pi]) \tag{14}$$

It can be clearly seen that the position at which the stress concentration factor presents depends on the far field loading style. In the polar coordinate system, the out-of-plane constrain factor is defined as follows

$$T_z = \frac{\bar{\sigma}_{zz}}{\nu(\bar{\sigma}_r + \bar{\sigma}_\theta)} \tag{15}$$

Substituting Eqs. (11), (A1) and (A2) into Eq. (15), then simplifying the resulting equation yields

$$\frac{1}{T_z} = \frac{A - A_2}{A} - \frac{1}{r^2 K_2(\sqrt{A}r)} \frac{A_2 c_{22}}{A\, c_{32}} + \frac{\nu(\sigma_x^\infty + \sigma_y^\infty)}{A K_2(\sqrt{A}r)(\cos 2\theta + t \sin 2\theta) c_{32}} \tag{16}$$

When the plate thickness is vanishing, this problem becomes a plane stress problem and the solutions to the in-plane stress field can be expressed as follows

$$\begin{aligned}
\sigma_r &= \left(1 - \frac{R^2}{r^2}\right)\frac{\sigma_x^\infty + \sigma_y^\infty}{2} + \left(1 - 4\frac{R^2}{r^2} + 3\frac{R^4}{r^4}\right)\left(\tau_{xy}^\infty \sin 2\theta + \frac{\sigma_x^\infty - \sigma_y^\infty}{2}\cos 2\theta\right) \\
\sigma_\theta &= \left(1 + \frac{R^2}{r^2}\right)\frac{\sigma_x^\infty + \sigma_y^\infty}{2} - \left(1 + 3\frac{R^4}{r^4}\right)\left(\tau_{xy}^\infty \sin 2\theta + \frac{\sigma_x^\infty - \sigma_y^\infty}{2}\cos 2\theta\right) \\
\tau_{r\theta} &= \left(1 + 2\frac{R^2}{r^2} + 3\frac{R^4}{r^4}\right)\left(\tau_{xy}^\infty \cos 2\theta - \frac{\sigma_x^\infty - \sigma_y^\infty}{2}\sin 2\theta\right)
\end{aligned} \tag{17}$$

Consider a special case that there is only one uni-axial load $\sigma_y^\infty = \sigma_0$ loading at far field. Now the tangential stress ratio becomes $K = \bar{\sigma}_\theta / \sigma_0$, which can be expressed as

$$K = \frac{1}{2}(1+\frac{R}{r^2}) + \cos 2\theta \left[\frac{1}{2} + g_1 \frac{A-A_2}{4\nu}\Big(K_0(\sqrt{A}r) + 2K_2(\sqrt{A}r) + K_4(\sqrt{A}r)\Big) + g_2\frac{6}{r^4}\right] \tag{18}$$

where

$$g_1 = \frac{4R\nu}{4\sqrt{A}K_1 + A_2R\left(2K_0 + \sqrt{A}RK_1\right)}$$
$$g_2 = R^3\frac{-4A^{3/2}RK_3 + A_2\left(\sqrt{A}R(4+AR^2)K_1 + 2(8+AR^2)K_2\right)}{16A^{3/2}K_1 + 4AA_2R\left(2K_0 + \sqrt{A}RK_1\right)} \tag{19}$$

The stress concentration factor for $r = R$ and $\theta = 0$ is

$$K_t = \frac{3}{2} + g_1\frac{A-A_2}{4\nu}(K_0 + 2K_2 + K_4) + g_2\frac{6}{R^4} \tag{20}$$

Eq. (16) can be rewritten as

$$\frac{1}{T_z} = \frac{A-A_2}{A} - \frac{1}{r^2K_2(\sqrt{A}r)}\frac{A_2}{A}\frac{c_{22}}{c_{32}} + \frac{\nu\sigma_0\sec 2\theta}{c_{32}AK_2(\sqrt{A}r)} \tag{21}$$

4. The three-dimensional stress field around the hole

4.1 The in-plane stress field

At first, the attention is placed on a special case- only a uni-axial load $\sigma_y^\infty = \sigma_0$ is loading at far field. Fig. 1 shows the distributions of the plane stress solution of σ_θ/σ_0 and the present solution of

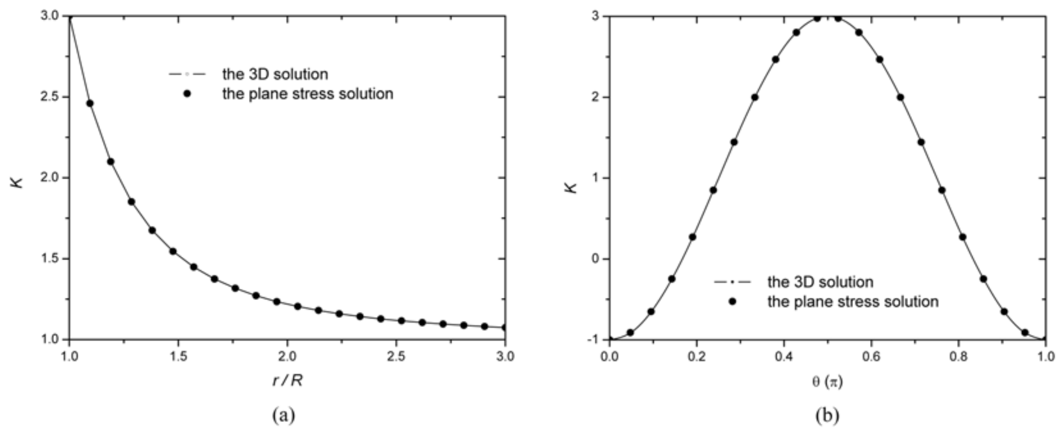

Fig. 1 Distributions of the plane stress solution of σ_θ/σ_0 and the 3D solution of tangential stress ratio $K = \bar{\sigma}_\theta/\sigma_0$ for cases that (a) on the section at $\theta = \pi/2$ and (b) at the line of $r/R = 1.0$ when $h/R = 0.01$ and $\nu = 1/3$

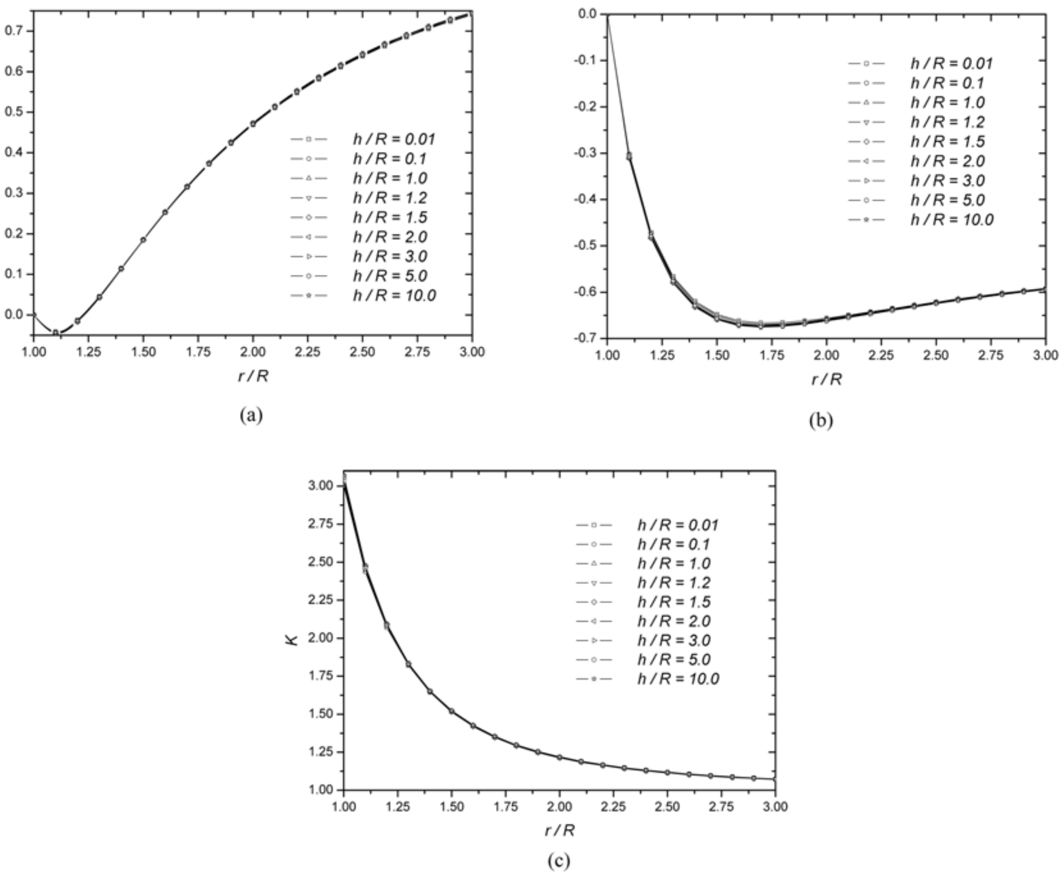

Fig. 2 Distributions of the three in-plane stress ratios: (a) $\bar{\sigma}_r/\sigma_0$ on the section at $\theta = 0$, (b) $\bar{\sigma}_{r\theta}/\sigma_0$ on the section at $\theta = \pi/4$ and (c) $K = \bar{\sigma}_\theta/\sigma_0$ on the section at $\theta = \pi/2$ with the distance ratio r/R for cases of $h/R = 0.01$, 0.1, 1.0, 1.2, 1.5, 2.0, 3.0, 5.0, 10.0 and $\nu = 1/3$

tangential stress ratio $K = \bar{\sigma}_\theta/\sigma_0$ on the section of $\theta = \pi/2$ and along the line of $r/R = 1.0$ for the case of $h/R = 0.01$ and $\nu = 1/3$. As is expected, the present solution for the case of a very thin plate coincides well with the relative plane stress solutions, completely. From Fig. 1(a), it can be found that σ_θ/σ_0 and K decrease rapidly from 3.0 and 3.00165 to 1.51852 when r/R varies from 1.0 to 1.5, respectively, then approach slowly and gradually to the limit value of 1.0. Fig. 1(b) shows that these two ratios increase monotonically from −1.0 and −1.00165 to 3.0 and 3.00165 when θ varies from 0 to $\pi/2$, respectively.

The variations of the three in-plane stress ratios with the distance ratio r/R on three different sections for various semi-thickness ration h/R are given in Fig. 2. From Fig. 2 it can be found that the variations of the three in-plane stress ratios are nearly independent of the thickness of the plate and are in good agreement with the related plane stress solutions. This conclusion is in good agreement with the results obtained by using the finite element method (Li *et al.* 2000, 2001).

Comparison of the present solutions with the related solutions given by Kotousov and Wang (2002a) is shown for the variation of the stress concentration factor, K_t, with the semi-thickness ratio h/R for different ν in Fig. 3. It can be found that the present solutions coincide very well with

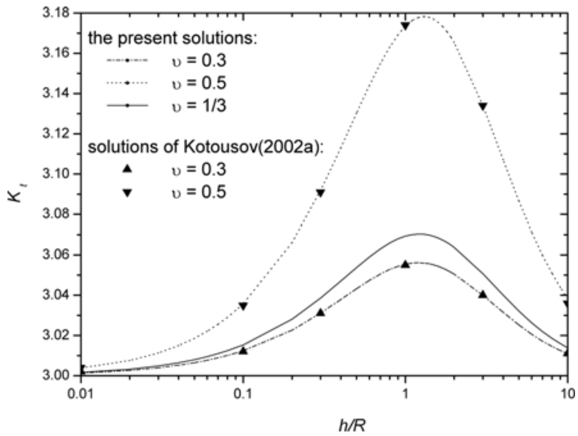

Fig. 3 Variations of the stress concentration factor K_t at the root of the circular hole with the semi-thickness ratio h/R for different ν

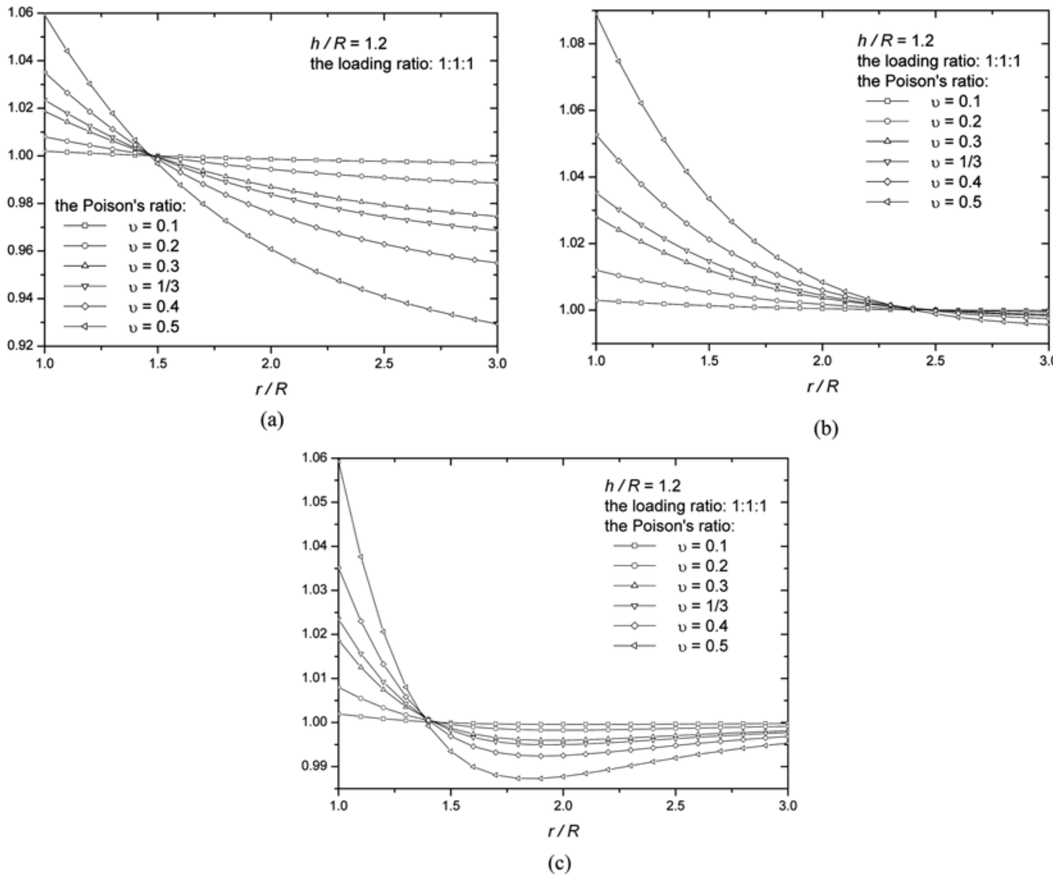

Fig. 4 Distributions of the three in-plane normalized stresses: (a) $\bar{\sigma}_r/\sigma_r$ on the section at $\theta = 3\pi/4$, (b) $\bar{\sigma}_{r\theta}/\sigma_{r\theta}$ on the section at $\theta = \pi/2$ and (c) $\bar{\sigma}_\theta/\sigma_\theta$ on the section at $\theta = 3\pi/4$ with the distance ratio r/R for different ν with $h/R = 1.2$ when the loads ratio is 1:1:1

that of Kotousov and Wang (2002a) completely. It also can be seen that both the plate thickness and Poisson's ratio have an obvious effect on the stress concentration. The stress concentration factor is higher in finite thickness plates than in thin plates of the plane stress and plane strain cases. The factor K_t rises quickly and reaches its peak value at about $h/R = 1.2$ when the plate is thin. Outside this region, K_t decreases with the increase of h/R. Based on the above results and comparison with some related for a special case of uni-axial load, it shows that the present solutions are valid.

Then, our attention is placed on the comparisons of the present 3D in-plane stress solutions with the related 2D solutions to show their deviations through Fig. 4. It shows distributions of the three in-plane normalized stresses with the distance ratio r/R and various Poisson's ratios ν for the cases of $h/R = 1.2$ and the loads ratio of 1:1:1. One should be mentioned that, the values of $\overline{\sigma}_r/\sigma_r$ and $\overline{\sigma}_{r\theta}/\sigma_{r\theta}$ at $r/R = 1.0001$ is looked as that at $r/R = 1.0$ for the analytic simplification. And emphasis is only placed on special section, on which stress components will easily reach their peak value. It is found that deviations of three in-plane stresses, $\overline{\sigma}_r$, $\overline{\sigma}_{r\theta}$ and $\overline{\sigma}_\theta$, increase with the increase of Poisson' ratio ν, and that they reach 5.924%, 8.888% and 5.926%, respectively, at the surface of the hole when $\nu = 0.5$. The deviation of the 3D solutions for the in-plane stress components is obvious due to the effect of the plate thickness and Poisson's ratio, although this effect on distributions of these three stress components is slight according to present solutions. Furthermore, the effect of Poisson's ratio is more significant than that of plate thickness.

4.2 The stress concentration and out-of-plane stress constraint effect

In this section, one studies the stress concentration first. Fig. 5 describes variations of the stress concentration factor K_t at the root of the circular hole with the semi-thickness ratio h/R. It can be seen from Fig. 5(a) that the plate thickness has an obvious effect on the stress concentration. The stress concentration factor is higher in finite thickness plates than that in the case of the plane stress and plane strain. The factor K_t rises quickly when the plate is relatively thin and reaches its peak value at about $h/R = 1.2$. Outside this region, K_t decreases with the increase of h/R and approaches its limit value. From Fig. 5(b), it can be seen that K_t depends strongly on the loads ratio.

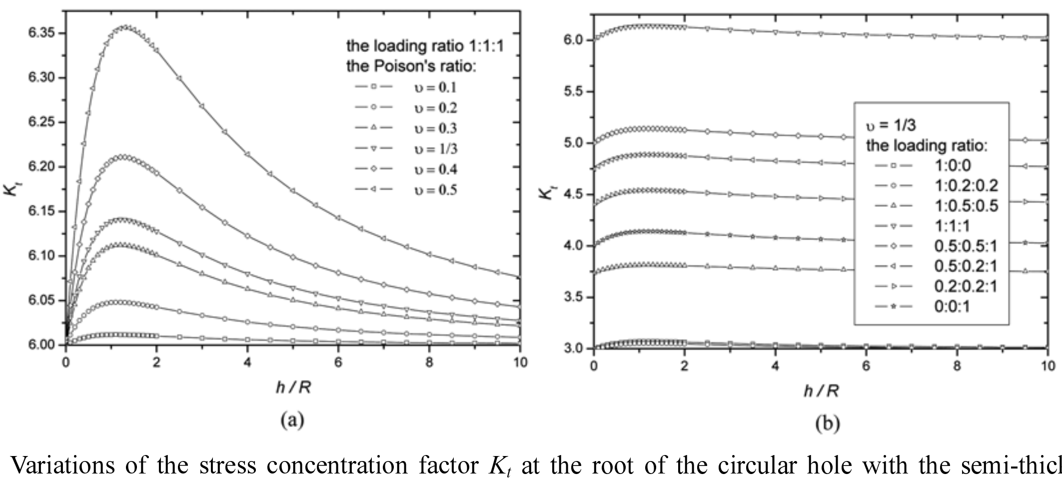

Fig. 5 Variations of the stress concentration factor K_t at the root of the circular hole with the semi-thickness ratio h/R for the case that (a) for different Poisson's ratio ν when the loads ratio is 1:1:1 (b) for different loads ratio with $\nu = 1/3$

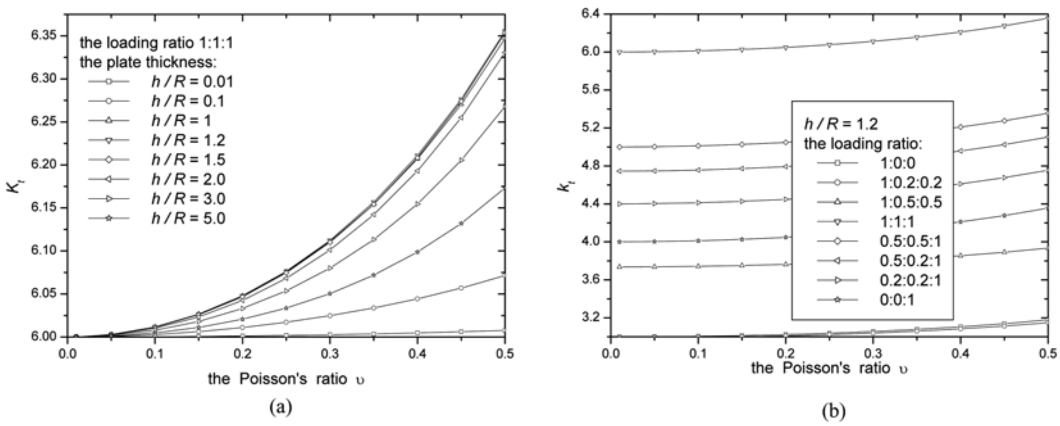

Fig. 6 Variations of the stress concentration factor K_t at the root of the circular hole with the Poison's ratio ν for the case that (a) for different plate thickness ratio when the loads ratio is 1:1:1 (b) for different loads ratio with $h/R = 1.2$

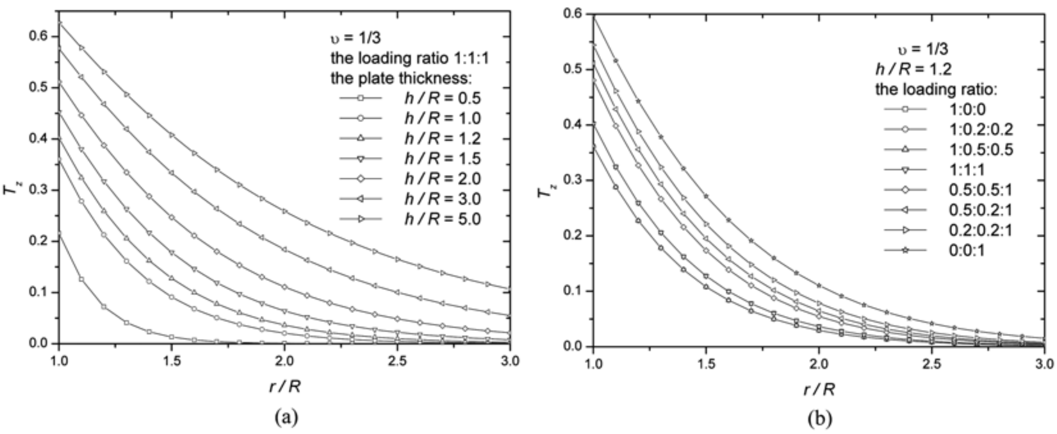

Fig. 7 Distributions of the out-of-plane stress constrain factor $T_z = \bar{\sigma}_{zz}/\nu(\bar{\sigma}_r + \bar{\sigma}_\theta)$ with the distance ratio r/R for the cases that (a) for different h/R with $\nu = 1/3$ when the loads ratio is 1:1:1 and (b) for different loads ratio with $\nu = 1/3$ and $h/R = 1.2$

Fig. 6 gives variations of the stress concentration factor K_t with Poison's ratio ν. It can be seen that K_t increases monotonically with ν and that K_t increase more rapidly when $h/R \approx 1.2$ than all other cases. Consequently, the maximum deviation of the present solution from the related plane stress solution is at $h/R \approx 1.2$ and $\nu = 0.5$. And the maximum deviation is about 5.926% when the loads ratio is 1:0:0, and 8.889% when the loads ratio is 0:0:1, respectively.

Next, the analysis is performed on the out-of-plane stress constraint effect. Distributions of the out-of-plane stress constrain factor T_z with the distance ratio r/R is shown in Fig. 7 when $\nu = 1/3$. Variations of the out-of-plane constrain factor T_z with the semi-thickness ratio h/R is plotted in Fig. 8. It shows that T_z increases with the increase of plate thickness and the decrease of the distance, and that the effect of the load ratio on the out-of-plane stress constraint is significant, especially when only the shear stress is loaded at far field. The value of T_z for an infinite thickness

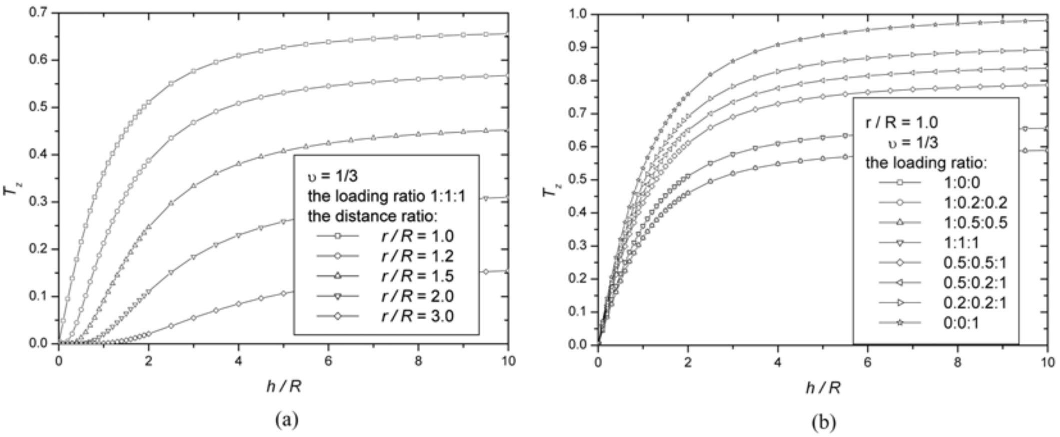

Fig. 8 Variations of the out-of-plane constrain factor $T_z = \bar{\sigma}_{zz}/\nu(\bar{\sigma}_r + \bar{\sigma}_\theta)$ with the semi-thickness ratio h/R for the cases that (a) for different r/R with $\nu = 1/3$ when the loads ratio is 1:1:1 and (b) for different loads ratio with $\nu = 1/3$ and $r/R = 1.0$

plate is about 2/3 when the loads ratio is 1:0:0, and 1 when the loads ratio is 0:0:1, respectively. It should be note that the effect of Poisson's ratio ν on T_z is rather weak on the section at $\theta = \theta_t$.

5. Conclusions

Based on Kane and Mindlin's assumption, theoretical solutions of the three-dimensional stress field are obtained for an infinite plate holding a through-the-thickness circular hole subjected to far field in-plane loads. Explicit expressions for the tangential stress around the hole and the out-of-plane stress constraint factor are obtained. Based on the present solutions, a comprehensive analysis is performed on the characters of 3D stress field and the emphasis has been placed on the effects of the plate thickness, Poisson's ratio and the load ratios on in-plane stress field, stress concentration and out-of-plane constraint. Some important characters are revealed:

(1) The dangerous position, where the failure of the plate will most likely take place initially, is determined by Eq. (14), the value of the tangential stress at this position is determined by Eq. (13), and the out-of-plane constrain factor is determined by Eq. (16).

(2) The effect of the plate thickness and Poisson's ratio on the deviation of the 3D in-plane stress components is obvious and could not be ignored, although this effect on distributions and variations of these three stress components is slight. Furthermore, the effect of Poisson's ratio is more significant than that of plate thickness. However, just on the contrary of that of the above two, the effect of the loads ratio on distributions and variations of the three in-plane stresses is significant, although this effect on the deviation degree of them from the related plane stress solutions is rather weak.

(3) The stress concentration factor rises quickly when the plate is relatively thin and reaches its peak value at about $h/R = 1.2$. Outside this region, it decreases with the increase of the plate thickness and approaches its limit value. And the stress concentration factor increases monotonically with the increase of Poisson's ratio. Furthermore, it increases more rapidly for the case of $h/R \approx 1.2$ than that of all other cases. The dependence between the stress

concentration factor and the load ratios is very strong. Consequently, the peak value of the factor occurs at $h/R \approx 1.2$ and $\nu = 0.5$. The maximum deviation of the present solution from the related plane stress solution is about 8.9% when the loads ratio is 0:0:1.

(4) The out-of-plane constraint factor increases with the increase of plate thickness and the decrease of the distance, and the effect of the load ratio on the out-of-plane constraint is significant. The factor can reach 1 at the surface of the hole when only the shear stress is loaded at far field. However, the effect of Poisson's ratio on the out-of-plane constraint is rather weak on the section at $\theta = \theta_t$.

Acknowledgements

The authors are grateful for financial supported by the National Natural Science Foundation of China (NSFC) (50675100). LD also thanks the Young Scientist Project of NSFC (041301060) for the support of this research.

References

Chaudhuri, R.A. (2003a), "Three-dimensional asymptotic stress field in the vicinity of the circumferential line of intersection of an inclusion and plate surface", *Int. J. Fract.*, **119**, 195-222.

Chaudhuri, R.A. (2003b), "Three-dimensional asymptotic stress field in the vicinity of the line of intersection of a circular cylindrical through/part-through open/rigidly plugged hole and a plate", *Int. J. Fract.*, **122**, 65-88.

Filippi, S., Lazzarin, P. and Tovo, R. (2002), "Developments of some explicit formulas useful to describe elastic stress fields ahead of notches in plates", *Int. J. Solids Struct.*, **39**, 4543-4565.

Filippo, B., Lazzarin, P. and Wang, C.H. (2004), Three-dimensional linear elastic distributions of stress and strain energy density ahead of V-shaped notches in plates of arbitrary thickness", *Int. J. Fract.*, **127**, 265-281.

Folias, E.S. (1975), "On the three-dimensional theory of cracked plates", *J. Appl. Mech.*, ASME, **42**, 663-674.

Folias, E.S. and Wang, J.J. (1990), "On the three-dimensional stress field around a circular hole in a plate of arbitrary thickness", *Comput. Mech.*, **6**, 379-391.

Jin, Z.H. and Hwang, K.C. (1989), "An analysis of three-dimensional effects near the tip of a crack in an elastic plate", *Acta. Mech. Solida Sin.,* **2**, 387-401.

Jin, Z.H. and Batra, R.C. (1997), "A crack at the interface between a Kane-Mindlin plate and a rigid substrate", *Eng. Fract. Mech.*, **57**, 343-354.

Kane, T.R. and Mindlin, R.D. (1956), "High-frequency extensional vibrations of plates", *J. Appl. Mech.*, ASME, **23**, 277-283.

Krishnaswamy, S., Jin, Z.H. and Batra, R.C. (1998), "Stress concentration in an elastic Cosserat plate undergoing extensional deformations", *J. Appl. Mech.*, ASME, **65**, 66-70.

Kotousov, A. (2007), "Fracture in plates of finite thickness", *Int. J. Solids Struct.*, **44**, 8259-8273.

Kotousov, A. and Wang, C.H. (2002a), "Three-dimensional stress constraint in an elastic plate with a notch", *Int. J. Solids Struct.*, **39**, 4311-4326.

Kotousov, A. and Wang, C.H. (2002b), "Three-dimensional solutions for transversally isotropic plates", *Compos. Struct.*, **57**, 445-452.

Kotousov, A. and Wang, C.H. (2002c), "Fundamental solutions for the generalized plane strain theory", *Int. J. Eng. Sci.*, **40**, 1775-1790.

Lazzarin, P. and Tovo, R. (1996), "A unified approach to the evaluation of linear elastic stress fields in the neighborhood of cracks and notches", *Int. J. Fract.*, **78**, 3-19.

Li, Z. and Guo, W. (2001), "Three-dimensional elastic stress fields ahead of blunt V-notches in finite thickness plates", *Int. J. Fract.*, **107**, 53-71.

Li, Z., Guo, W. and Kuang, Z. (2000), “Three-dimensional elastic stress fields near notches in finite thickness plates”, *Int. J. Solids Struct*., **37**, 7617-7631.
Penado, F.E. and Folias, E.S. (1989), “The three-dimensional stress field around a cylindrical inclusion in a plate of arbitrary thickness”, *Int. J. Fract*., **39**, 129-146.
Sadowsky, M.A. and Sternberg, E. (1949), Stress concentration around an ellipsoidal cavity”, *J. Appl. Mech*., ASME, **16**, 149-157.
Sternberg, E. and Sadowsky, M.A. (1949), “Three-dimensional solution for the stress concentration around a circular hole in a plate of arbitrary thickness”, *J. Appl. Mech*., ASME, **16**, 27-38.
Yang, J. and Guo, S. (2005), “On using the Kane-Mindlin theory in the analysis of crack in plates”, *Int. J. Fract*., **133**, L13-L17.
Yang, W. and Freund, L.B. (1985), “Transverse shear effects for through-crack in an elastic plate”, *Int. J. Solids Struct*., **21**, 977-994.
Yang, Z., Kim, C.B., Cho, C. and Beom, H.G. (2008), “The concentration of stress and strain in finite thickness elastic plate containing a circular hole”, *Int. J. Solids Struct*., **45**, 713-731.
Young, C.K. and Sternberg, E. (1966), “Three-dimensional stress concentration around a cylindrical hole in a semi-infinite elastic body”, *J. Appl. Mech*., ASME, **33**, 855-865.

Appendix

$$
\begin{aligned}
\overline{\sigma}_r = & \frac{A_2\left(-2c_{10}Ar^2 - c_{20}Ar^2(2\ln r - 1) + 4c_{30}\sqrt{A}rK_1(\sqrt{A}r)\right)}{4Ar^2\nu} \\
& + \frac{A_2\sin 2\theta}{Ar^2\nu}\left[-Ac_{21} + c_{31}\left(\sqrt{A}rK_1(\sqrt{A}r) + 6K_2(\sqrt{A}r)\right)\right] \\
& + \frac{A_2\cos 2\theta}{Ar^2\nu}\left[-Ac_{22} + c_{32}\left(\sqrt{A}rK_1(\sqrt{A}r) + 6K_2(\sqrt{A}r)\right)\right] + \frac{\nu d_{20} - c_{30}\sqrt{A}rK_1(\sqrt{A}r)}{r^2\nu} \\
& - \frac{\sin 2\theta}{r^4\nu}\left[c_{31}r^2\left(\sqrt{A}rK_1(\sqrt{A}r) + 6K_2(\sqrt{A}r)\right) + 2\nu(r^4d_{11} + 3d_{21})\right] \\
& - \frac{\cos 2\theta}{r^4\nu}\left[c_{32}r^2\left(\sqrt{A}rK_1(\sqrt{A}r) + 6K_2(\sqrt{A}r)\right) + 2\nu(r^4d_{12} + 3d_{22})\right]
\end{aligned}
$$

$$
\begin{aligned}
\overline{\sigma}_\theta = & -\frac{A_2\left[2c_{10} + c_{20}(1 + 2\ln r)\right]}{4\nu} - \frac{d_{20}}{r^2} + \frac{c_{30}(A - A_2)}{\sqrt{A}r\nu}\left(\sqrt{A}rK_0(\sqrt{A}r) + K_1(\sqrt{A}r)\right) \\
& + \frac{\sin 2\theta}{\nu r^4}\left\{c_{31}r\frac{A - A_2}{A\sqrt{A}}\left[\sqrt{A}r\left(6 + Ar^2\right)K_0(\sqrt{A}r) + 3\left(4 + Ar^2\right)K_1(\sqrt{A}r)\right] + 2\nu\left(r^4d_{11} + 3d_{21}\right)\right\} \\
& + \frac{\cos 2\theta}{\nu r^4}\left\{c_{32}r\frac{A - A_2}{A\sqrt{A}}\left[\sqrt{A}r\left(6 + Ar^2\right)K_0(\sqrt{A}r) + 3\left(4 + Ar^2\right)K_1(\sqrt{A}r)\right] + 2\nu\left(r^4d_{12} + 3d_{22}\right)\right\}
\end{aligned}
$$

$$
\begin{aligned}
\overline{\sigma}_{r\theta} = & \frac{A_2\cos 2\theta}{2Ar^2\nu}\left[Ac_{21} - 4c_{31}\left(\sqrt{A}rK_1(\sqrt{A}r) + 3K_2(\sqrt{A}r)\right)\right] \\
& + \frac{A_2\sin 2\theta}{2Ar^2\nu}\left[-Ac_{22} + 4c_{32}\left(\sqrt{A}rK_1(\sqrt{A}r) + 3K_2(\sqrt{A}r)\right)\right] \\
& + \frac{2\cos 2\theta}{r^4\nu}\left[c_{31}r^2\left(\sqrt{A}rK_1(\sqrt{A}r) + 3K_2(\sqrt{A}r)\right) - d_{11}r^4\nu + 3\nu d_{21}\right] \\
& - \frac{2\sin 2\theta}{r^4\nu}\left[c_{32}r^2\left(\sqrt{A}rK_1(\sqrt{A}r) + 3K_2(\sqrt{A}r)\right) - d_{12}r^4\nu + 3\nu d_{22}\right]
\end{aligned}
$$

$$
\overline{\sigma}_z = A\left[c_{30}K_0(\sqrt{A}r) + \left(c_{31}\sin 2\theta + c_{32}\cos 2\theta\right)K_2(\sqrt{A}r)\right]
$$

$$
\begin{aligned}
\overline{\sigma}_{zr} = & \frac{c_{20}}{r} - c_{30}\sqrt{A}K_1(\sqrt{A}r) - \frac{\sin 2\theta}{r^3}\left[2c_{21} + c_{31}r^2\left(\sqrt{A}rK_1(\sqrt{A}r) + 2K_2(\sqrt{A}r)\right)\right] \\
& - \frac{\cos 2\theta}{r^3}\left(2c_{22} + c_{32}r^2\left[\sqrt{A}rK_1(\sqrt{A}r) + K_3(\sqrt{A}r)\right]\right)
\end{aligned}
$$

$$
\overline{\sigma}_{z\theta} = \frac{2}{r^3}\left[\cos 2\theta\left(c_{21} + c_{31}r^2K_2(\sqrt{A}r)\right) - \sin 2\theta\left(c_{22} + c_{32}r^2K_2(\sqrt{A}r)\right)\right] \tag{A1}
$$

where

$$
\begin{aligned}
&c_{20} = c_{30} = c_{11} = c_{12} = 0, \qquad c_{10} = -\frac{\nu\left(\sigma_x^\infty + \sigma_y^\infty\right)}{A_2}, \\
&d_{20} = -\frac{1}{2}R^2\left(\sigma_x^\infty + \sigma_y^\infty\right), \qquad d_{11} = -\frac{\tau_{xy}^\infty}{2}, \qquad d_{12} = \frac{1}{4}\left(-\sigma_x^\infty + \sigma_y^\infty\right) \\
&c_{21} = tc_{22}, \qquad c_{31} = tc_{32}, \qquad d_{21} = td_{22} \\
&c_{22} = -\frac{1}{2}R^2\left(\sqrt{A}RK_1 + 2K_2\right)c_{32} \\
&d_{22} = \left[\frac{1}{2}\sqrt{A}RK_1\left(A_2R^2 - 4\frac{A - A_2}{A}\right) + K_2\left(A_2R^2 - 8\frac{A - A_2}{A}\right)\right]\frac{R^2}{8\nu}c_{32} \\
&c_{32} = -\frac{8R\nu}{2RA_2K_0 + \sqrt{A}\left(4 + R^2A_2\right)K_1}\frac{\sigma_x^\infty - \sigma_y^\infty}{2}
\end{aligned}
\tag{A2}
$$

In which, K_n denotes $K_n(\sqrt{A}R)$, the modified Bessel functions of order n, where n is an integer, and

$$
t = \frac{2\tau_{xy}^\infty}{\sigma_x^\infty - \sigma_y^\infty} \tag{A3}
$$